Journal of Thermal Science Vol.29, No.4 (2020) 982–991

https://doi.org/10.1007/s11630-020-1336-9 **Article ID: 1003-2169(2020)04-0982-10**

Heat Transfer Performance of Microgroove Back Plate Heat Pipes with Working Fluid and Heating Power

WU Yanpeng[1*], JIA Jie[1], TIAN Dongmin[1], CHUAH Yew Khoy[2]

1. Department of Building Environment and Energy Engineering, University of Science and Technology Beijing, Beijing 100083, China
2. Department of Energy and Refrigerating Air Conditioning Engineering, Taipei University of Technology, Taipei 10608, China

Abstract: Micro heat pipes (MHP) cooling is one of the most efficient solutions to radiate heat for high heat flux electronic components in data centers. It is necessary to improve heat transfer performance of microgroove back plate heat pipes. This paper discusses about influence on thermal resistance through experiments and numerical simulation with different working fluids, filling ratio and heat power. Thermal resistance of the CO_2 filled heat pipe is 14.8% lower than the acetone filled heat pipe. In the meantime, at the best filling ratio of 40%, the CO_2 filled heat pipe has the optimal heat transfer behavior with the smallest thermal resistance of 0.123 K/W. The thermal resistance continues to decline but the magnitude of decreases is going to be minor. In addition, this paper illustrates methods about how to enhance heat pipe performance from working fluids, filling ratio and heat power, which provides a theoretical basis for practical applications.

Keywords: microgroove back plate heat pipes, working fluids, filling ratio, heat power

1. Introduction

With rapid growing of data centers and constant increment of high heat flux of electronic components [1, 2], traditional heat dissipation method is not powerful to meet the cooling requirement for computer rooms [3–5]. Micro heat pipe as the most effective component for cooling micro-scale electronic device, due to its simple structure, convenient operation and excellent thermal diffusivity and isothermally, becomes an important research hotspot currently [6–12].

Lips et al. [13] tested the heat transfer behavior of microgroove flat heat pipes with experiments and observed the nuclear boiling phenomenon through visualized experiments. Bai et al. [14] studied the effect of vacuum on the heat transfer performance of pulsating heat pipes with deionized water and Al_2O_3/H_2O nanofluids as working fluid. Qu et al. [15] investigated the start-up and heat transfer performance of pulsating heat pipes with different placement methods and volumetric liquid filling ratios. Kuang et al. [16] classified the factors affecting heat transfer performance of the groove micro-heat pipe and summarized influence of various factors on heat transfer performance. Hou et al. [17] analyzed the impact of liquid filling ratio and heating power on the heat transfer performance of two flat heat pipes with non-uniform groove structure. Fan et al. [18] observed the effects of rectangular and zigzag

Received: Sep 29, 2019 AE: MAHIAN Omid Corresponding author: WU Yanpeng E-mail: wuyanpeng@126.com

grooves flat heat pipes on the heat transfer performance with different filling ratios, working fluids and groove aspect ratio. Wang et al. [19] examined the heat transfer performance with different evaporation and condensation lengths of flat heat pipes. Wang et al. [20] designed a flat heat pipe with deep micro groove structure to see how placement influences the heat transfer performance. Chen et al. [21] obtained the liquid filling ratio of 25% for optimizing heat transfer performance of flat heat pipes with acetone as a working fluid. Peng et al. [22] studied the effect of the wind speed of the cold-end fan, the filling ratio of the working fluid and the degree of vacuum on the heat dissipation capability of the flat-plate heat pipe.

Above all, most papers demonstrate methods to strengthen the heat transfer coefficient by improving structures without filling the heat pipe with CO_2 as working fluids. This paper describes the comparison of two working fluids (CO_2 and acetone), analyzes the effect of filling ratio and heat power on the heat transfer performance of microgroove back plate heat pipes and offers the optimal value to increase the heat transfer performance.

2 Experimental Investigation

2.1 Experiments system

In order to test the heat transfer performance of microgroove back plate heat pipe, the testing bench (shown as Fig. 1) consists of heating system, heat pipe, cooling system and data collection system.

(1) Heating system

Heating system is used for simulating the work of server chips and collecting the energy during the work. It contains DC power supply, contact regulator, power meter and ceramic heater. The voltage is provided by DC power supply and changed to produce different thermal power by contact regulator when server is working. The power meter can read voltage and current of two ends of ceramic heater which converts electric energy into heat as the source of heat pipe and brings evaporation section heat. The one side of the ceramic heater has been linked to a microgroove back plate heat pipe through a thermal grease. This design lessens the effect of thermal contact resistance between the heat source and microgroove back plate heat pipes. Moreover, insulation materials cut off natural convection heat transfer between heat source and environment entirely.

(2) Heat pipe

Heat transfer system is mainly composed of heat transfer element microgroove back plate heat pipes, involving evaporator, adiabatic and condenser section. The length of three sections is 25 mm, 75 mm and 50 mm respectively. Fig. 2 shows the internal structure size of heat pipe. The top of the pipe has insulation materials which isolate the natural convection heat transfer with external factors and generate a perfect adiabatic condition while monitoring.

(3) Cooling system

Cooling system is for condensing gas phase as work fluids and taking away the heat absorbed by a heat pipe. The cooling system consists of cold plates, a peristaltic

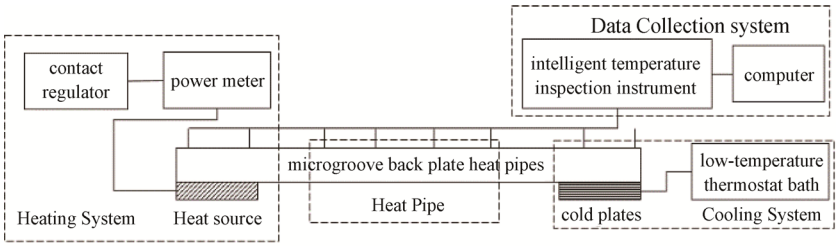

(a) Testing bench system

(b) Testing bench built for experiments

Fig. 1 Testing bench of microgroove back plate heat pipes

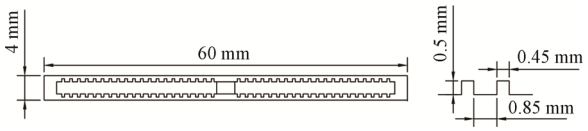

Fig. 2 The internal structure size of heat pipe

pump and a low-temperature thermostat bath. Set the temperature of low-temperature thermostat bath and start pump. When the velocity of water is stable, start the heating system. Cold plate is linked to the condensation section of a microgroove back plate through a thermal grease, which can reduce the contact resistance of cold plates.

(4) Data collection system

Temperature data of the microgroove back plate heat pipe are collected and stored by the data collection system, involving temperature sensors, an intelligent temperature inspection instrument and a computer. Temperature data from different locations of a heat pipe are tested by couples of temperature sensors and collected by the intelligent temperature inspection instrument, then stored in the computer while connecting to the instrument. T type thermocouple (TT-T-40) thermometers are used to set up on the heat pipes by a conductive gel. The numbers of thermocouples put at evaporator, adiabatic and condenser section are 2, 4 and 2 respectively. Fig. 3 shows the location distribution of T type thermocouples.

2.2 Data processing

Eq. (1) represents the thermal resistance related to the operated temperature difference between heat pipes and heating power. The smaller the thermal resistance, the better the heat transfer performance. In addition, the working fluids, the filling factor and heating power can affect the resistance.

$$R_{th} = \frac{T_e - T_c}{Q} \tag{1}$$

In Eq. (1), R_{th} is the thermal resistance of a heat pipe (K/W); T_e is the temperature of the evaporator (K); T_c is the temperature of the condenser (K); Q is the heating power of the heat pipe (W).

2.3 Error analysis

The uncertainty of temperature measurement is $U_{\Delta T} = \pm\frac{0.1}{15} = \pm 6.67\times10^{-3}$. The uncertainties of voltage and current are U_U=±5×10^{-3} and U_I=±5×10^{-3}, respectively [23].

$$\begin{aligned} Max.U_Q &= \pm\left(U_U^2 + U_I^2\right)^{1/2} \\ &= \pm 0.00707 \approx \pm 0.71\% \end{aligned} \tag{2}$$

$$\begin{aligned} Max.U_{R_{th}} &= \pm\left[U_{\Delta T}^2 + \left(-U_Q\right)^2\right]^{1/2} \\ &= \pm 0.00972 \approx \pm 0.97\% \end{aligned} \tag{3}$$

Therefore, uncertainties in power and thermal resistance are ±0.71% and ±0.97%, respectively.

2.4 Experimental results

2.4.1 Work fluids

Fig. 4 shows the temperature distribution along the bottom axial direction of a micro groove back plate heat pipe filled with CO_2 and acetone at a filling ratio of 30% and a heating power of 50 W. The temperature distribution of the two working fluids filled heat pipe is gradually reduced from the evaporator to the condenser. The temperature of the evaporator is the highest while the temperature of the condenser is the lowest. Average temperature of the evaporator of CO_2-filled heat pipe is 41.95 K lower than average temperature of evaporator of the acetone-filled heat pipe.

Table 1 shows the thermal resistance of a heat pipe filled with two different working fluids under the condition of 50 W heating power and 30% liquid filling ratio. Compared with acetone, the heat pipe has a smaller operated temperature difference and thermal resistance and a better heat transfer performance with CO_2 as filling fluids.

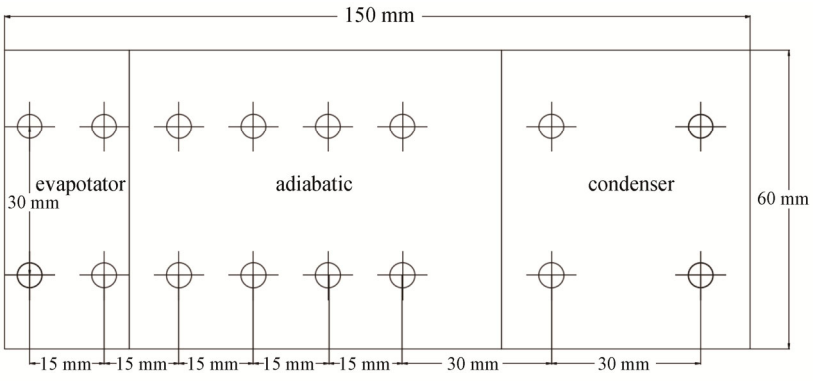

Fig. 3 Micro-groove back plate heat pipe temperature measuring point layout

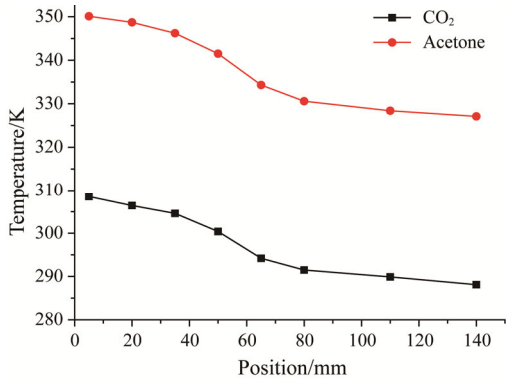

Fig. 4 Temperature distribution along axial direction of heat pipe with different working fluids

Table 1 Thermal resistances with different working fluids

Parameters and units		Working fluid	
		CO_2	Acetone
Evaporation section temperature	K	307.45	349.40
Condensation section temperature	K	289.00	327.75
Working temperature difference	K	18.45	21.65
Thermal resistance	K/W	0.369	0.433

The performance of heat pipes is totally different when the filled working fluids, the filling ratio and heating conditions are distinct. Experiments have been designed with two working fluids and filling ratio, and four levels to discuss the impact on thermal resistance. The best charging ratio of the micro groove back plate heat pipes is no more than 0.5 [24]. Generally, the heating power of CPU is 40 W. Table 2 shows experimental conditions.

As shown in Table 2, thermal resistance of the CO_2 filled heat pipe is lower. CO_2 filled heat pipe can improve the heat transfer performance and enhance the performance. Define R_j (j=1, 2) as the range (max-min value of thermal resistance) between each arithmetic mean value with different factors.

The influence degree of filling ratio and heating power on the CO_2 heat pipe can be judged by the range R value. The greater the range R value, the greater the influence on the thermal resistance. As shown in Fig. 5, the influence of liquid filling ratio on the thermal resistance of the heat pipe is less than that of heating power.

2.4.2 Filling ratio

Fig. 6 shows the temperature distribution along the bottom axial direction of a microgroove back plate CO_2 filled heat pipe at four different filling ratios. All of the temperature distribution at four different filling ratios are gradually reduced from evaporator to condenser, and the average temperature of evaporator reaches the highest at the filling ratio of 20%.

Table 2 Thermal resistances with different working fluids (2 factors & 4 levels)

No.	Filling Ratio/ %	Heat Power/ W	Thermal resistance (CO_2)/K·W^{-1}	Thermal Resistance (Acetone)/K·W^{-1}
1	20	30	0.723	1.158
2	20	40	0.519	0.987
3	20	50	0.378	0.801
4	20	60	0.322	0.546
5	30	30	0.698	0.814
6	30	40	0.484	0.604
7	30	50	0.369	0.433
8	30	60	0.299	0.331
9	40	30	0.648	0.902
10	40	40	0.465	0.724
11	40	50	0.357	0.527
12	40	60	0.286	0.428
13	50	30	0.662	1.042
14	50	40	0.478	0.857
15	50	50	0.359	0.610
16	50	60	0.295	0.436

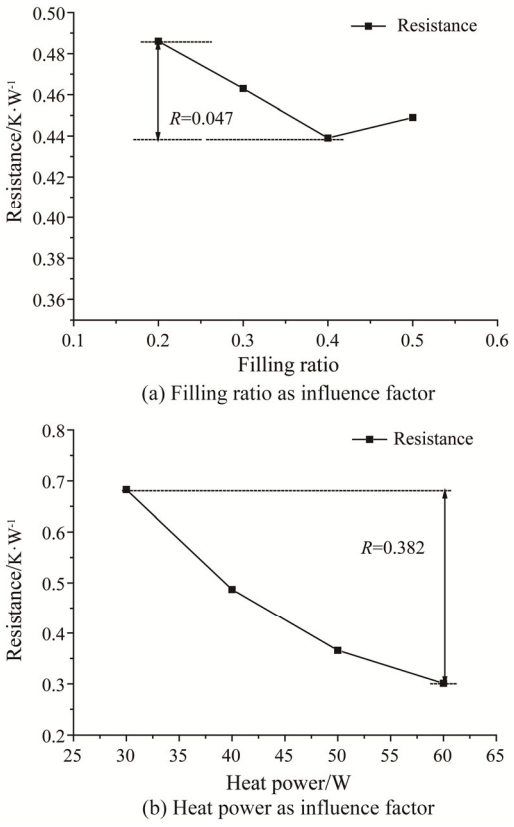

Fig. 5 The arithmetic mean value and the range with different factors and levels of CO_2 heat pipe

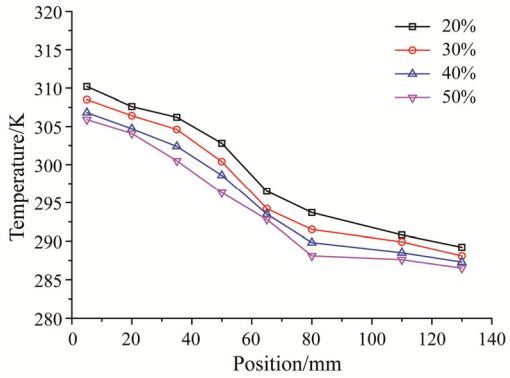

Fig. 6 The axial temperature of CO_2 heat pipe at different filling ratios

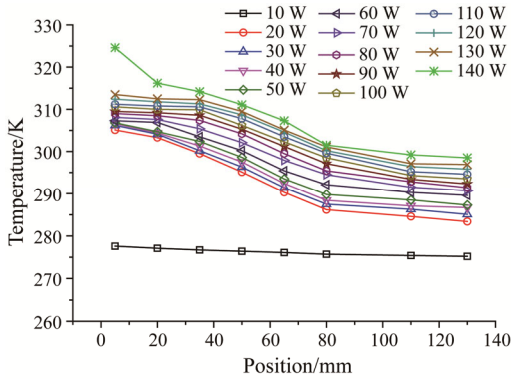

Fig. 7 The axial temperature of CO_2 heat pipe at different heating power

Table 3 shows the thermal resistances of a heat pipe with 50 W heating power and different filling ratios. The CO_2 filled heat pipe has a smaller operated temperature difference, a lower thermal resistance and a better heat transfer performance at the filling ratio of 40%.

Table 3 Thermal resistances of CO_2 heat pipes at different filling ratios

Parameters and units		Filling ratio			
		20%	30%	40%	50%
Evaporation section temperature	K	308.90	307.45	305.75	305.00
Condensation section temperature	K	290.00	289.00	287.90	287.05
Working temperature difference	K	18.90	18.45	17.85	17.95
Thermal resistance	K/W	0.378	0.369	0.357	0.359

2.4.3 Heating power

Fig. 7 shows temperature distribution along the bottom axial direction of a micro groove back plate CO_2 filled heat pipe at the filling ratio of 40% and heating power between 10 W and 140 W. The temperature distribution is gradually lessened from evaporator, adiabatic to condenser. With the increase of the heating power, the temperature of the whole heat pipe has been improved and the temperature difference of the heat pipe has been decreased gradually. However, the decreasing range of the temperature difference is getting smaller. Finally, there is no obvious change of the temperature difference. When the heating power is 10 W, the heat pipe has not been activated and the heat transfer is mainly coming from its own heat conduction without any phase changes. With the improvement of heating power, working fluid starts phase change. The increasing temperature of the evaporation section accelerates vaporizing process gradually and reduces the thermal resistance. When the heating power reaches 140 W, the working fluids in the evaporator steam too fast and the temperature is not stable.

3. Numerical Simulation

3.1 Physical models and boundary conditions

This paper uses the software FLUENT to process the numerical simulation of the heat transfer of the microgroove back plate heat pipe. Since the microgroove back plate heat pipe can occur phase changes and it is hard to build a 3D physical model with intensive computation and the problem of divergence, a 2D physical model has been built with the simplification of the heat pipe. As shown in Fig. 8, the 2D model is the axial section of a real microgroove back plate heat pipe, and also consists of evaporator, adiabatic and condenser section. The length of three sections is 25 mm, 75 mm, and 50 mm respectively. In Fig. 8, x_{hp} represents the length of the heat pipe; y_{hp} represents the thickness of the heat pipe; and y_f represents the height of the fluid. Therefore, y_f/y_{hp} in this model represents the liquid filling ratio of the heat pipe. By changing y_f/y_{hp}, different liquid filling ratio of heat pipes can be studied.

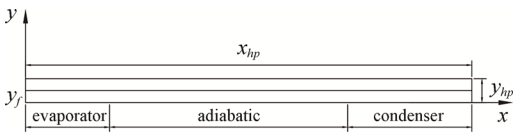

Fig. 8 Physical model of microgroove back plate heat pipe

Table 4 shows mesh independency test result. Based on the simplified rectangular model, 11250 quadrilateral meshes are chosen. When the number of nodes is 11250, relative errors of different nodes are less than 0.6%.

Table 4 Mesh independency test result

Number of nodes	Thermal resistance/K·W^{-1}	Relative error
11250	0.675	——
17578	0.674	0.148%
45000	0.671	0.593%

The left and right wall surfaces, the upper wall surface and the adiabatic section are both adiabatic boundaries, and the heat flux density of them is 0. The evaporation section has a constant heat flux density boundary, which is determined by the heating power and the cross-sectional area of the heat pipe. The boundary of the condensation section has a fixed convection heat transfer coefficient indicated by the heat dissipation of the heat pipe.

The governing equations consist of continuity equation (Eq. (4)), N-S equation (Eq. (5)) and energy conservation equation (Eq. (6)). In Eq. (4), S_M is the mass source term (kg/(m^3·s)), and is calculated by Eq. (10). In Eq. (5), p is the static pressure (Pa); τ_{ij} is the stress tensor and is calculated by Eq. (7). In Eq. (6), S_E is the energy source term (kg/(m^3·s)), and is calculated by Eq. (8) and Eq. (9). In Eq. (8), β_e is the evaporating coefficient; α_{liq} is the liquid volume fraction; ρ_{liq} is the liquid phase density (kg/m^3). In Eq. (9), β_c is the condensation coefficient; α_{vap} is the gas volume fraction; ρ_{vap} is the gas phase density (kg/m^3). And the sum of α_{liq} and α_{vap} is 1.

$$\frac{\partial \rho}{\partial t}+\frac{\partial}{\partial x_i}\left(\rho u_i\right)=S_M \tag{4}$$

$$\frac{\partial\left(\rho u_i\right)}{\partial t}+\frac{\partial}{\partial x_j}\left(\rho u_i u_j\right)=-\frac{\partial p}{\partial x_i}+\frac{\partial \tau_{ij}}{\partial x_j}+\rho g_i+F_i \tag{5}$$

$$\begin{aligned}&\frac{\partial\left(\rho S_E\right)}{\partial t}+\frac{\partial}{\partial x_i}\left[u_i\left(\rho S_E+p\right)\right]\\&=\frac{\partial}{\partial x_j}\left[\left(k_{ij}+\frac{C_p \mu_t}{Pr_t}\right)\frac{\partial T}{\partial x_j}+u_i \tau_{ij}\right]+S_M\end{aligned} \tag{6}$$

$$\tau_{ij}=\mu_{eff}\left(\frac{\partial u_j}{\partial x_i}+\frac{\partial u_i}{\partial x_j}\right)-\frac{2}{3}\mu_{ij}\frac{\partial u_i}{\partial x_i}\delta_{ij} \tag{7}$$

$$S_E=-\beta_e \alpha_{liq}\rho_{liq}\left|\frac{T_{liq}-T_{sat}}{T_{sat}}\right|\Delta H \tag{8}$$

$$S_E=\beta_c \alpha_{vap}\rho_{vap}\left|\frac{T_{vap}-T_{sat}}{T_{sat}}\right|\Delta H \tag{9}$$

$$S_M=\beta_e \alpha_{liq}\rho_{liq}\left|\frac{T_{liq}-T_{sat}}{T_{sat}}\right| \tag{10}$$

3.2 Simulation results

3.2.1 Working fluids

Fig. 9 shows the simulated temperature distribution along the bottom axial direction of a micro groove back plate heat pipe filled with CO_2 and acetone at a liquid filling ratio of 30% and a heating power of 50 W. Both of the temperature constantly decreases from evaporator to condenser. The average temperature value of the evaporator filled with CO_2 is lower than the value of the pipe filled with acetone.

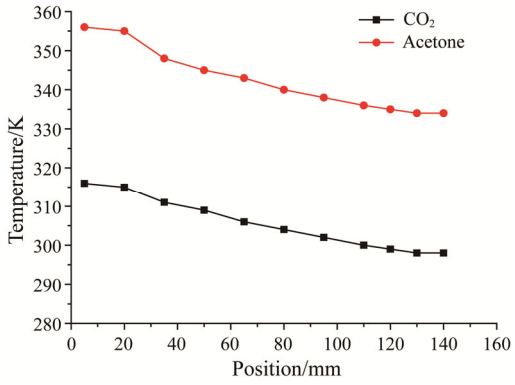

Fig. 9 The axial temperature of heat pipes at different working fluid

After further processing with simulated temperature data, the thermal resistances have been computed and listed as Table 5 with two working fluids at filling ratio of 30% and heat power of 50 W. The thermal resistance of heat pipe filled with CO_2 is 0.335 K/W while the thermal resistance of heat pipe filled with acetone is 0.415 K/W. Therefore, the heat transfer performance of the heat pipe can be enhanced with CO_2 as working fluids.

Table 5 Thermal resistances of heat pipes with different working fluids

Parameters and units		Working fluid	
		CO_2	Acetone
Evaporation section temperature	K	315.50	355.50
Condensation section temperature	K	298.75	334.75
Working temperature difference	K	16.75	20.75
Thermal resistance	K/W	0.335	0.415

Through 16 types of operating conditions with different heat power and filling ratios, the thermal resistances under each condition are computed and illustrated as Table 6. The results demonstrate a lower thermal resistance has been achieved with CO_2 as working fluids compared with acetone as working fluids.

3.2.2 Filling ratio

The impact on the heat transfer performance of microgroove back plate heat pipes is simulated with the CO_2 as working fluids and 50 W power heat and at filling ratio of 20%, 30%, 40% and 50%, respectively. After 60 s modelling, the internal operating condition of the heat pipe is nearly stable.

The temperature simulation results along the bottom axial direction of the heat pipe with the microgroove back plate are shown in Fig. 10. The temperature

Table 6 Thermal resistances of heat pipes with different working fluids

No.	Filling ratio/%	Heat power/W	Thermal resistance (CO_2)/K·W^{-1}	Thermal resistance (Acetone)/K·W^{-1}
1	20	30	0.675	1.035
2	20	40	0.488	0.842
3	20	50	0.375	0.623
4	20	60	0.304	0.497
5	30	30	0.633	0.714
6	30	40	0.444	0.541
7	30	50	0.335	0.415
8	30	60	0.271	0.322
9	40	30	0.592	0.821
10	40	40	0.406	0.635
11	40	50	0.315	0.446
12	40	60	0.258	0.339
13	50	30	0.608	0.913
14	50	40	0.419	0.704
15	50	50	0.320	0.511
16	50	60	0.263	0.358

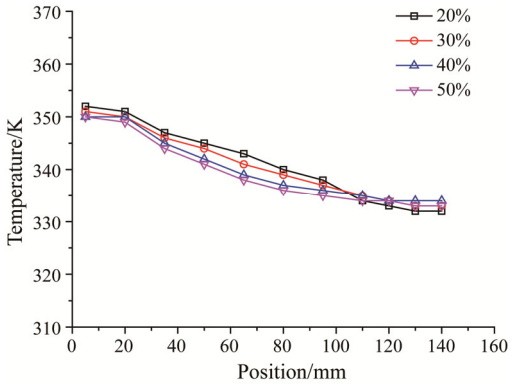

Fig. 10 The axial temperature of CO_2 heat pipes at different filling ratios

distribution of the microgroove back plate heat pipe under four different liquid filling ratios decreased gradually from the evaporator to the condenser. The average temperature of the evaporator of heat pipe with the liquid filling ratio of 20% is the highest.

The thermal resistances of the heat pipe with microgroove back plate with working fluid of CO_2 and filling ratio of 20%, 30%, 40% and 50% under the condition of heating power of 50 W, are shown in Table 7. When the working medium of the heat pipe is CO_2 and the liquid filling ratio is 40%, the working temperature difference of the heat pipe is smaller; the thermal resistance is smaller; and the heat exchange effect is better.

Table 7 Thermal resistances of CO_2 heat pipes with different heat filling ratios

Parameters and units		Filling ratio			
		20%	30%	40%	50%
Evaporation section temperature	K	316.50	315.50	315.00	314.50
Condensation section temperature	K	297.75	298.75	299.25	298.50
Working temperature difference	K	18.75	16.75	15.75	16.00
Thermal resistance	K/W	0.375	0.335	0.315	0.320

3.2.3 Heating power

Simulation of the effect of CO_2 filled and 20%, 30%, 40% and 50% liquid filling ratio on the heat transfer performance of microgroove back plate heat pipe with heating power of 20 W, 30 W, 40 W, 50 W and 60 W. After 60 s of numerical simulation, the working fluid inside the heat pipe almost reached a stable working state.

The temperature simulation results along the bottom axial direction of the heat pipe with the microgroove back plate are shown in Fig. 11. The temperature distribution of microgroove back plate heat pipe with different liquid filling ratio under different heating power decreases gradually from the evaporator to the condenser, with the highest temperature in the evaporator and the lowest temperature in the condenser. With the increase of heating power, the temperature inside the heat pipe also increases.

The thermal resistances of microgroove backboard heat pipes with different liquid filling ratios (20%, 30%, 40% and 50%) under different heating power are shown in Fig. 12.

With the increase of heating power, the thermal resistance of the heat pipe with different liquid filling ratio decreases gradually, but the decrease amplitude is smaller and smaller. Finally, with the increase of heating power, the thermal resistance almost has no obvious change. With the increase of heating power, the faster the working medium absorbs heat in the evaporator, the faster the working medium accumulates heat, the faster the temperature on the wall of the heat pipe rises, which accelerates the flow of the working medium, and the driving force of the flow in the heat pipe is larger, so the thermal resistance of the heat pipe decreases greatly with the increase of heating power. However, the total amount of working medium in the heat pipe is certain. Therefore, if the heating power continues to increase, the thermal resistance of the heat pipe changes less and less, and the thermal resistance of the heat pipe also tends to be stable.

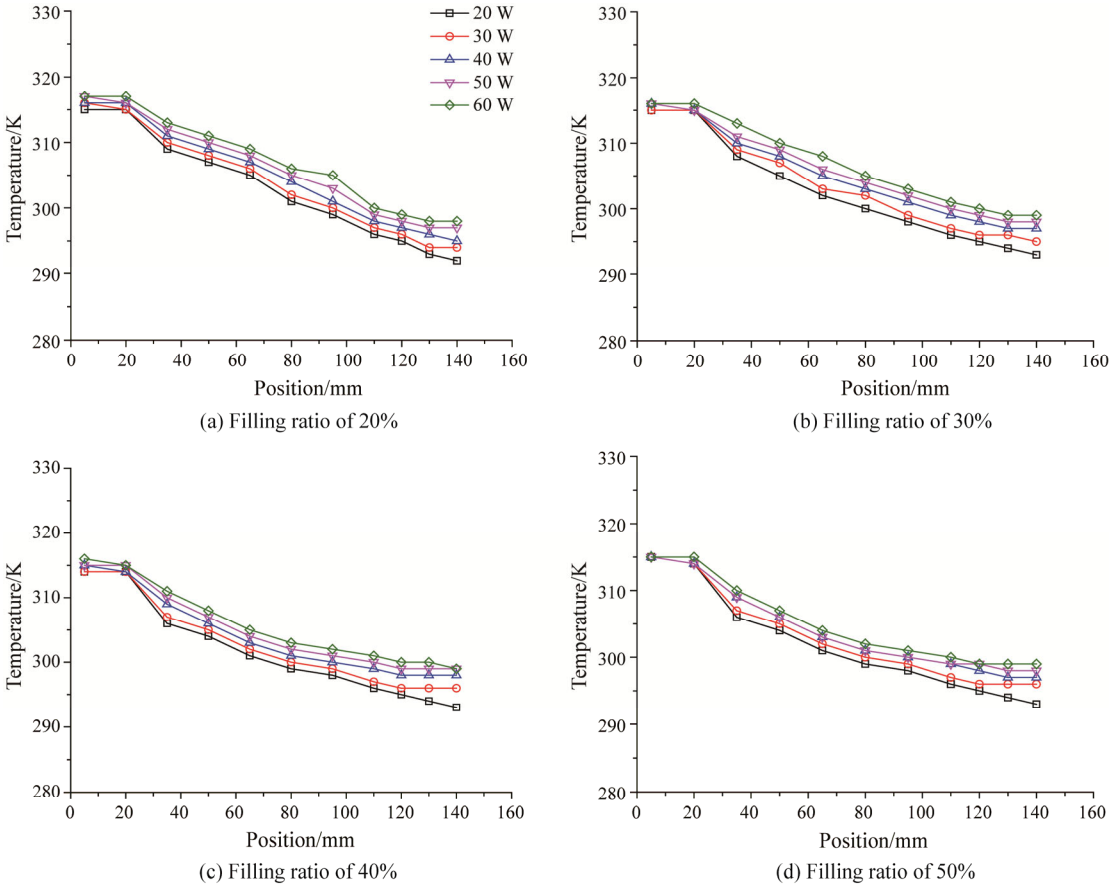

Fig. 11 The axial temperature of CO_2 heat pipes at different filling ratios

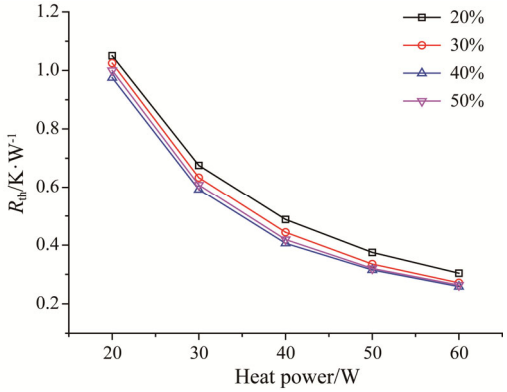

Fig. 12 Thermal resistance diagram with different filling ratios of CO_2 heat pipes

3.3 Comparison of the experimental results and the simulation results

The experimental results and simulation results of heat pipe surface temperature distribution under different parameters are compared. Although there is a gap between the two data, the temperature distribution trend is consistent. The thermal resistance of the heat pipe between the experimental results and the simulation results is compared. As shown in Table 8, there is a

Table 8 Comparison of heat pipe thermal resistance test results and simulation results

No.	Experimental thermal resistance/ K·W^{-1}	Simulated thermal resistance /K·W^{-1}	Percentage of error/%
1	0.723	0.675	7.11
2	0.519	0.488	6.35
3	0.378	0.375	0.80
4	0.322	0.304	5.92
5	0.698	0.633	10.27
6	0.484	0.444	9.01
7	0.369	0.335	10.15
8	0.299	0.271	10.33
9	0.648	0.592	9.46
10	0.465	0.406	14.53
11	0.357	0.315	13.33
12	0.286	0.258	10.85
13	0.662	0.608	8.88
14	0.478	0.419	14.08
15	0.359	0.320	12.19
16	0.295	0.263	12.17

certain gap between the experimental results and the simulation results, but the gap is less than 15%.

4. Conclusions

This paper draws the following conclusions on the microgroove back plate heat pipes by doing experiments and numerical simulation. Experimental and simulated temperature distribution trend are consistent.

(1) Different working fluids affect the heat transfer performance of heat pipes. With same filling ratio and heat power, the CO_2 filled heat pipe has lower thermal resistance and better heat transfer performance than the pipe filled with acetone.

(2) The filling ratio has a large impact on the heat transfer performance of heat pipes. There exists a greatest filling ratio for microgroove back plate heat pipes with CO_2 as working fluids. And when filling ratio is 40%, the heat transfer performance of the heat pipe reaches the peak with the lowest thermal resistance of 0.123 K/W.

(3) The heat transfer performance of heat pipes is affected by the heat power. A certain starting power power lies in the microgroove back plate heat pipe filled with CO_2. As the heat power is rising, the thermal resistance is gradually decreasing with declined amplitude of range variation.

Acknowledgements

The authors gratefully acknowledge the financial support for this research through the Beijing Natural Science Foundation (No. 8202034) and the USTB-NTUT Joint Research Program.

References

[1] Gu L.J., Yang H.W., Hu S., US data center energy saving experience and enlightenment. China Energy, 2015, 37(06): 26–29+21. (in Chinese)

[2] Noie S.H., Heat transfer characteristics of a two-phase closed thermo syphon. Applied Thermal Engineering, 2005, 25(4): 495–506.

[3] Elnaggar H.A., Abdullah M.Z., Mujeebu M.A., Experimental analysis and FEM simulation of finned U-shape multi heat pipe for desktop PC cooling. Energy Conversion and Management, 2011, 52: 2937–2944.

[4] Elnaggar H.A., Abdullah M.Z., Mujeebu M.A., Characterization of working fluid in vertically mounted finned U-shape twin heat pipe for electronic cooling. Energy Conversion and Management, 2012, 62: 31–39.

[5] Rao Z.H., Wang S.F., Wu M.H., Lin Z.R., Li F.H., Experimental investigation on thermal management of electric vehicle battery with heat pipe. Energy Conversion and Management, 2013, 65: 92–97.

[6] Vasiliev L.L., Heat pipes in modern heat exchangers. Applied Thermal Engineering, 2005, 25(1): 1–19.

[7] Wang Y., Vafai K., An experimental investigation of the thermal performance of an asymmetrical flat plate heat pipe. International Journal of Heat and Mass Transfer, 2000, 43(15): 2657–2668.

[8] Hsieh S.S., Lee R.Y., Shyu J.C., Chen S.W., Thermal performance of flat vapor chamber heat spreader. Energy Conversion and Management, 2008, 49(6): 1774–1784.

[9] Hsieh S.S., Yang Y.R., Design, fabrication and performance tests for a polymer based flexible flat heat pipe. Energy Conversion and Management, 2013, 70: 10–19.

[10] Hsieh S.S., Lee R.Y., Shyu J.C., Chen S.W., Analytical solution of thermal resistance of vapor chamber heat sink with and without pillar. Energy Conversion and Management, 2007, 48(10): 2708–2717.

[11] Hamideh S., Saeed Z.H., Ali A., Mohammad P.F., Experimental investigation of a novel type of two-phase closed thermo syphon filled with functionalized carbon nanotubes/water nanofluids for electronic cooling application. Energy Conversion and Management, 2019, 188: 321–332.

[12] Noie S.H., Heris S.Z., Kahani M., et al, Heat transfer enhancement using Al_2O_3/water nanofluid in a two-phase closed thermo syphon. International Journal of Heat and Fluid Flow, 2009, 30(4): 700–705.

[13] Lips S., Lefèvre F., Bonjour J., Nucleate boiling in a flat grooved heat pipe. International Journal of Thermal Sciences, 2009, 48(7): 1273–1278.

[14] Bai L.N., Su X.J., Ren W.H., Yang W.Z., Effect of vacuum on heat transfer performance of pulsating heat pipe. Cryogenics and Superconductivity, 2019, 47(04): 62–66. (in Chinese)

[15] Qu J., Peng Y.Q., Sun Q., Heat transfer characteristics of compact three-dimensional pulsating heat pipe with flat evaporator. Journal of Chemical Engineering, 2018, 69(07): 2899–2907. (in Chinese)

[16] Kuang X., Wei W., Yang W., Xie X.Z., Hu W. Study on factors affecting heat transfer performance of groove micro heat pipes. Low temperature and superconductivity, 2018, 46(03): 58–63. (in Chinese)

[17] Hou Y.P., Cui W.Z., Nie X., Xie Z.W., Experimental study on heat transfer performance of non-uniform groove flat heat pipe. Journal of Chongqing University, 2018, 41(03): 13–20. (in Chinese)

[18] Fan C.L., Qu W., Sun F.R., Experimental study on heat transfer performance of three kinds of microgroove

structure flat heat pipes. Electronic Devices, 2003, 26(4): 357–360. (in Chinese)

[19] Wang S., Chen J., Hu Y., et al., Effect of evaporation section and condensation section length on thermal performance of flat plate heat pipe. Applied Thermal Engineering, 2011, 31(14): 2367–2373.

[20] Wang C., Liu Z.L., Zhang G.M., et al., Experimental study on the influence of tilt angle on the performance of flat plate heat pipe. Journal of Engineering Thermophysics, 2012, 33(008): 1400–1402. (in Chinese)

[21] Chen J.S., Chou J.H., Cooling performance of flat plate heat pipes with different liquid filling ratios. International Journal of Heat and Mass Transfer, 2014, 77: 874–882.

[22] Peng H., Li J., Ling X., Study on heat transfer performance of an aluminum flat plate heat pipe with fins in vapor chamber. Energy Conversion and Management, 2013, 74: 44–50.

[23] Heris S.Z., Edalati Z., Noie S.H., et al., Experimental investigation of Al_2O_3/Water Nanofluid through equilateral triangular duct with constant wall heat flux in laminar flow. Heat Transfer Engineering, 2014, 35(13): 1173–1182.

[24] Zhao Y.H., Wang H.Y., Diao Y.H., Wang X.Y., Deng Y.C., Flat plate micro heat pipe array and its heat transfer characteristics. Journal of chemical industry, 2011, 62(02): 336–343. (in Chinese)